

A High-Order Unstructured Mixed Method for Aerodynamic Applications

Min Kyu Jung¹ and *Oh Joon Kwon¹

¹Department of Aerospace Engineering, KAIST, Korea.

*Corresponding author: ojkwon@kaist.ac.kr

Abstract

A flow solver based on a mixed mesh paradigm is developed for resolving flows in a high-order accurate manner. The proposed mesh topology involves unstructured tetrahedral/prismatic mesh in the near-body region and adaptive Cartesian-based unstructured mesh in the off-body region. The body-conforming near-body unstructured mesh offers a great flexibility in treating complex geometries, and also ensures proper mesh resolution for capturing the boundary layer. For the Cartesian mesh in the off-body region, a high-order accurate WENO scheme was adopted to better resolve the detailed flow features. A multi-level mesh adaptation scheme with a tree-based data structure was also employed directly on the Cartesian cells to further enhance the accuracy of the solution. To transfer the flow information between the two mesh topologies, an overset mesh technique was applied. The accuracy and performance of the flow solver were validated for fixed-wing and rotary-wing configurations.

Keywords: Mixed Unstructured Mesh, Overset Mesh, High-order WENO scheme, Adaptive Mesh Refinement

Introduction

Accurate prediction of unsteady flow fields around rotorcrafts still remains as one of the most challenging problems in the field of applied aerodynamics. One of the key aspects of the rotorcraft flow simulation is in the accurate capturing of near-field rotor wake that has significant impacts on the blade aerodynamic loading, overall vehicle performance, vibration, and noise (Datta et al., 2008; Caradonna et al., 1988; Harihanan et al., 2012). At the same time, prediction of the unsteady off-body phenomena, such as the far-wake development, vortex or pressure wave propagation, and their interactions with other bodies, is also very critical. Therefore, to accurately assess the aerodynamic performance of rotorcrafts, elaborate flow simulations are required, along with an ability of handling complex geometric configurations and the relative motion between the rotorcraft sub-components.

The main difficulty involved in the rotorcraft aerodynamic simulations is in the fact that the trailed tip vortices typically have very small core size, and convect over a relatively long distance (Pulliam et al., 2009). To capture these tip vortices accurately with less numerical dissipation at given order of accuracy of the scheme, dense cells need to be distributed along their trajectories. However, this may result in a very large number of cells, and thus require an excessive computational cost. To avoid this problem, solution-adaptive mesh refinement methods based on feature detection techniques, so-called h-adaptation, are sometimes adopted to locally enhance the density of the grids (De Zeeuw, 1993; Kamkar et al., 2011). However, this may be a difficult task for structured grids because of the regularity of the point distribution. Thus, on the structured mesh frameworks, mesh adaptation is usually performed on block or patch bases. Meanwhile, for unstructured mesh topologies, direct cell-based mesh adaptation is easily applicable. Another approach of better resolving the tip vortices and avoiding excessive numerical dissipation is to use high-order accurate numerical schemes, sometimes coupled with solution-adaptive mesh refinement/coarsening.

To overcome the shortcomings of using single mesh strategies and to achieve high-order accuracy, dual-mesh methods have been proposed. The OVERFLOW solver has been developed by adopting structured body-fitted grids in the near-body region, and multi-level Cartesian grids in the off-body

region (Buning, 2003). The two grid zones are coupled with an overset mesh scheme by using a domain connectivity module. OVERFLOW adopts spatial accuracy up to sixth-order using central differencing and allows adaptive mesh refinement by a multi-block approach. The solver offers good computational results, but the geometry modeling with structured body-fitted grids is still difficult and is time-consuming, particularly for complex configurations. Recently, the Helios flow solver has been developed based on a hybrid grid paradigm by adopting unstructured meshes in the near-body region to allow more flexible geometry modeling (Wissink et al., 2008). Helios employs coupling of a set of several existing codes, the parallel unstructured mesh NSU3D flow solver for the near-body region and the serial high-order structured ARC3D flow solver for the solution on the Cartesian grids at the off-body region, through a Python infrastructure (Mavriplis et al., 1997; Hornung et al., 2006; Pulliam, 1984; Schluter et al., 2005). The CHIMPS software is used for the communication between the overlapped two mesh systems. While the flux calculation in the near-body unstructured mesh region is performed with second-order accuracy, high-order accuracy is achieved up to sixth-order in the off-body Cartesian grid region. Even though the flow solver was successfully used for solving several rotor flow problems, the file-based data exchange between the two independent heterogeneous mesh solvers is known to degrade the solution efficiency and the parallel scalability of the coupled solver. Also, mesh adaptation in the off-body Cartesian mesh region can be achieved only by multi-block bases because of the nature of the structured grids.

In the present study, a new mixed-type unstructured mesh flow solver is developed for solving flows around fixed- and rotary-wing configurations in a high-order accurate manner. The proposed mixed mesh paradigm involves prismatic/tetrahedral unstructured mesh in the near-body region and adaptive Cartesian-based unstructured mesh in the off-body region. The two mesh domains are coupled using an overset mesh topology. Unlike the Helios flow solver, the present flow solver is implemented by adopting a same unstructured mesh finite-volume topology, and thus is a unified solver. In the off-body Cartesian mesh region, to better resolve the detailed flow features away from the body, a high-order WENO scheme was achieved by utilizing the regularity of the Cartesian mesh cells. Also, a multi-level tree-based mesh adaptation scheme was employed directly on cells to further enhance the accuracy of the solution in the Cartesian mesh region. In the near-body prismatic/tetrahedral mesh region, second-order accuracy was maintained. The flow solver was validated against the NACA0015 wing in a steady flow condition and the Caradonna-Tung rotor in a hovering flight condition. The results were compared with the available experimental data, and the effect of the order of accuracy in the flow solution was discussed.

Numerical Method

The fluid motion is modeled by the three-dimensional, compressible Reynolds-averaged Navier-Stokes equations. The equations can be written in an integral form for arbitrary computational domain V with boundary ∂V as

$$\iint_{\Omega} \frac{\partial}{\partial t} \bar{Q} dV + \oint_{\partial\Omega} (\bar{F} \cdot \bar{n}) dS = \oint_{\partial\Omega} (\bar{G} \cdot \bar{n}) dS + \iint_{\Omega} S dV \quad (1)$$

where \bar{Q} is the vector of the primitive variables, and $\bar{F}(Q)$ and $\bar{G}(Q)$ denote the inviscid and viscous fluxes of these variables, respectively. The governing equations were discretized using a vertex-centered finite-volume method in the near-body region. In the off-body Cartesian mesh region, a cell-centered scheme was applied. The convective flux term was evaluated by employing the flux-difference splitting scheme of Roe, whereas the diffusive flux term was computed by adopting a modified central-difference method. An implicit time integration algorithm based on a linearized second-order Euler backward differencing coupled with dual-time stepping was used to advance the solution in time. The linear system of equations was solved at each time step using a

point Gauss-Seidel method. The Spalart-Allmaras one-equation turbulence model was adopted to consider the turbulent eddy viscosity in the calculations.

Near-Body Flow Solver

For the near-body region, body-fitted unstructured tetrahedral and prismatic unstructured mesh is constructed. This mesh offers the flexibility of treating complex geometries and resolving the viscous shear layers, such as the boundary layers. In this near-body region, a vertex-centered finite-volume method is adopted. The flow domain is divided into a finite number of control volumes surrounding each vertex, which are made of non-overlapping median-dual cells. For the inviscid flux calculations, a second-order spatial accuracy is achieved through a linear reconstruction procedure based on either the least-square method or the Green-Gauss reconstruction technique. To achieve numerical stability along the steep gradient region, such as the shock discontinuities, a slope limiter proposed by Venkatakrisnan was adopted.

Off-Body Flow Solver

The off-body region is modeled with unstructured Cartesian mesh generated by a tree-data structure. In the present study, the volume mesh generation in the off-body region is conducted by a simple and robust procedure of cell division. Starting with a coarse background mesh or a single root cell, hexahedral elements are repeatedly subdivided to resolve emerging features of the flow (Aftosmis, 1997). The off-body region is discretized by using a cell-centered finite-volume method to comply with the regularity and the orthogonality of Cartesian meshes. The flow calculation is performed in a high-order accurate manner by adopting WENO (Weighted Essentially Non-Oscillatory) scheme to better resolve the detailed flow features. WENO scheme utilizes the weights of sub-stencils based on the local smoothness of the numerical solution to automatically achieve high-order accuracy and non-oscillatory approximation of the solution around flow discontinuities. To further enhance the accuracy of the flow solution, a solution-adaptive mesh refinement/coarsening methodology is also applied in the off-body region. In the present study, two types of feature detection method were adopted. To capture the flow discontinuities such as the shock and the contact surface, the total velocity difference was applied, while the non-dimensional Q-criterion was utilized for vortex-driven flows (De Zeeuw, 1993; Kamkar et al., 2011).

Results and Discussion

The present flow solver was applied to typical fixed-wing and rotary wing configurations, and the effects of the order of accuracy and the mesh adaptation on the results are discussed. The order of accuracies tested are the second-order adopting a least-square method, and the third-, fifth-, and seventh-order WENO schemes. The results with and without the adaptive mesh refinement were also compared.

Steady Flow around an NACA0015 Wing

A steady flow around an NACA 0015 rectangular wing was simulated to compare the tip vortex resolution by adopting the high-order scheme and the solution adaptive mesh refinement. The present test case was experimentally studied at a freestream Mach number of 0.1235, a Reynolds number of 1.5 million, and a positive angle of attack of 12 degrees (McAllister and Takahashi, 1991). The wing has an aspect ratio of 3.3 with a square tip.

Figure 1 shows the predicted wake structures for the different order of accuracies represented by the iso- λ_2 surface colored by vorticity magnitude. The minimum cell size is $\Delta x = 0.05c$, and the small cells are initially clustered around the wing and the vortex shedding region. It is shown that in the cases of second- and third-order accurate solutions, the tip vortices are evolved from the wing tips, but are quickly diffused due to numerical dissipation. On the other hand, the numerical results of the

fifth- and seventh-order WENO schemes show that the tip vortices are well-developed to further downstream and the strength is well maintained along the fine cells. To quantify the difference of the wake resolution by the order of accuracy, non-dimensional z -direction velocity distributions are presented at two- and six-chord lengths downstream of the trailing edge in Fig. 2. The results are compared with the experimental data. It is shown that improved velocity distributions are obtained with high-order schemes by better preserving the wake structure, even though the numerical solutions are not close enough to the experimental data.

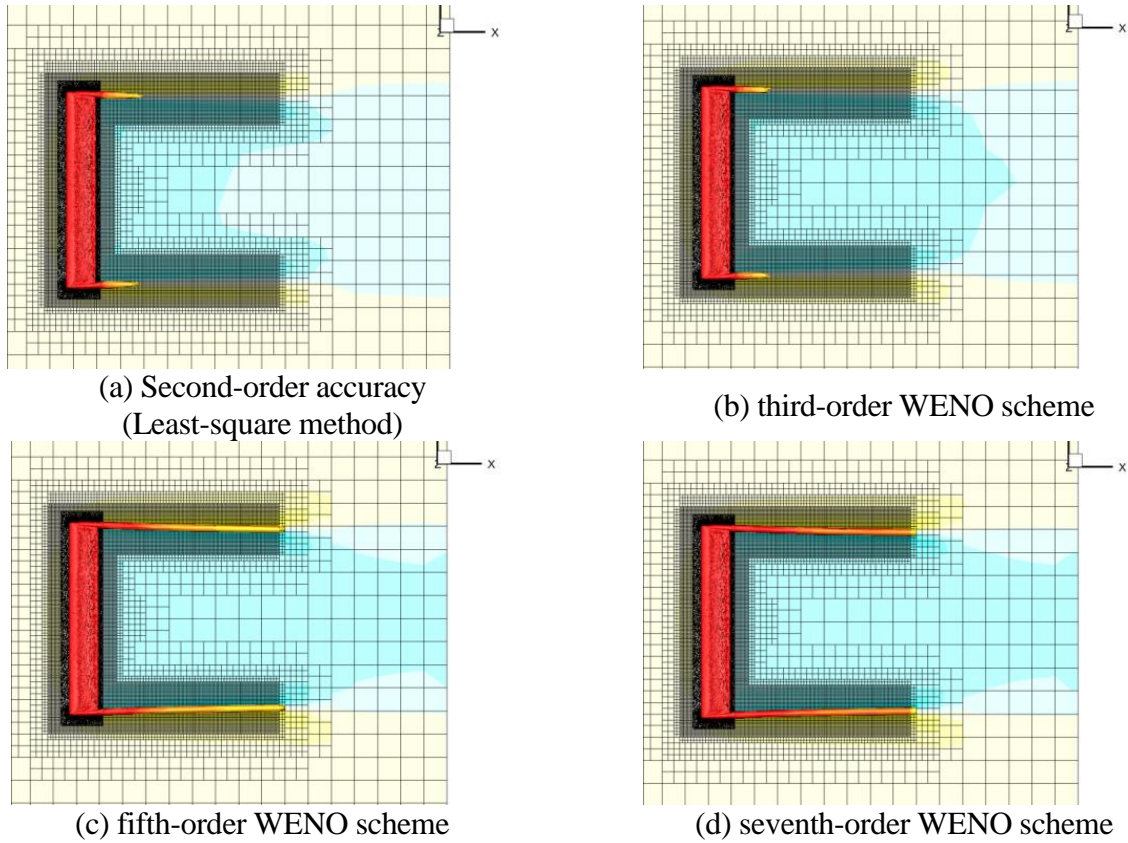


Figure 1. Wake structure represented by iso- λ_2 surface for NACA 0015 Wing. (a) L-S method; (b) WENO3; (c) WENO5; (d) WENO7.

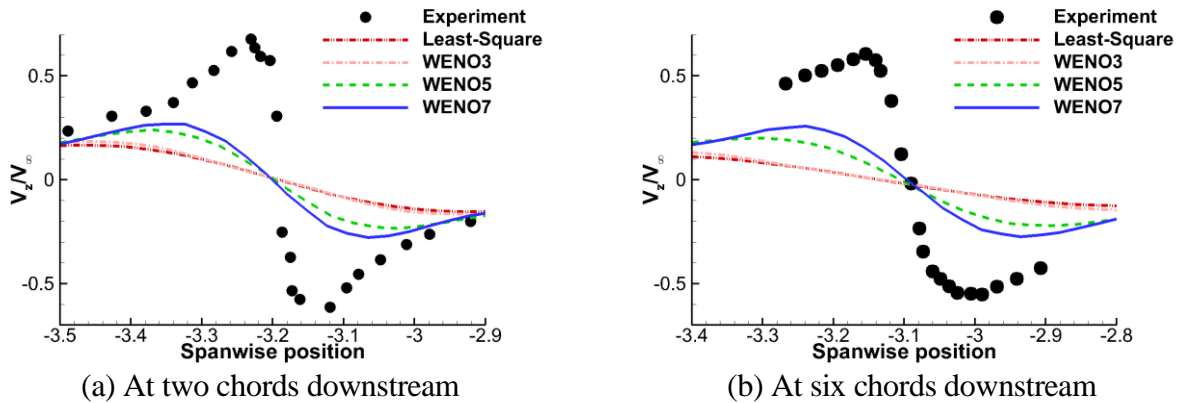


Figure 2. Comparison of normalized z -directional velocity distributions in wake region for NACA 0015 wing. (a) Two chords from trailing edge; (b) Six chords from trailing edge.

To further enhance the flow resolution of the tip vortex, the solution-adaptive mesh refinement was performed by using the non-dimensional Q-criterion. The wake structures are represented by the iso- λ_2 surface for the initial and adaptive meshes in Fig. 3. The results of seventh-order accuracy previously shown in Fig. 1 were utilized as the baseline solution for the mesh adaptation. The additional flow calculation was performed by maintaining the same seventh-order accuracy, and the mesh adaptation was conducted up to the second refinement level such that the typical cell size becomes $\Delta x = 0.0125c$. It is shown in Fig. 3 that the mesh adaptation was well implemented along the downstream from the wing tip, and the tip vortices are preserved better until they reach the downstream boundary. In Fig. 4, the resultant normalized z -direction velocity distributions are presented, along with the experiment and the Helios prediction (Wissink et al, 2010). The Helios is a hybrid mesh flow solver which uses sixth-order central difference with $\Delta x = 0.025c$ grid spacing in the off-body. Both numerical results show similar velocity distributions, but the adaptive mesh solution shows better resolution by employing the higher order scheme and more fine meshes. It is shown that the adaptive mesh refinement additionally improves the flow resolution significantly, demonstrating that for accurate flow simulations a proper mesh resolution is also essential in addition to high-order accurate numerical schemes.

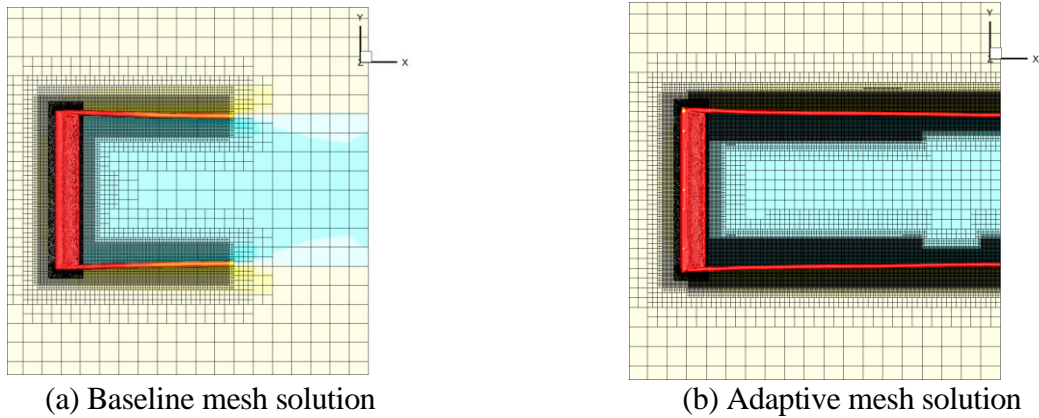


Figure 3. Wake structure for NACA 0015 Wing with 7th-order accuracy. (a) Baseline mesh solution; (b) Adaptive mesh solution.

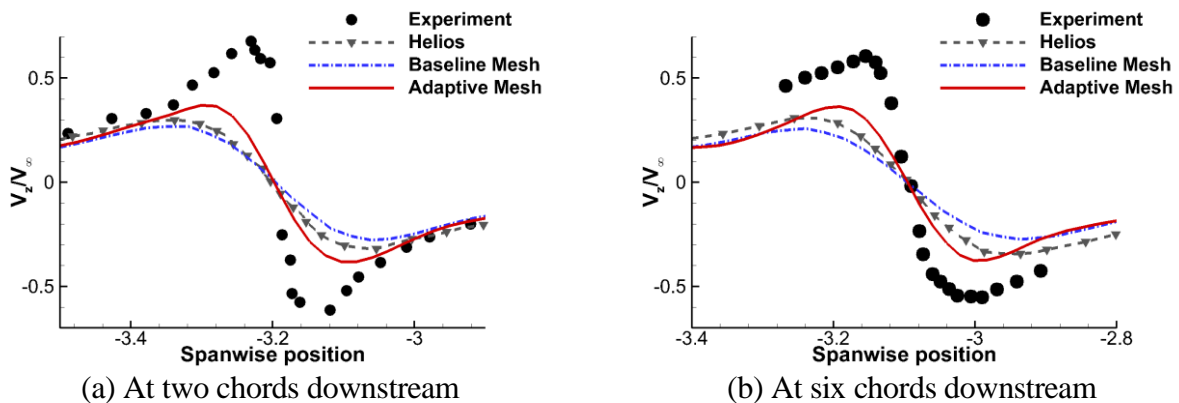


Figure 4. Effect of mesh adaptation on normalized z -directional velocity distributions for NACA 0015 wing. (a) Two chords from trailing edge; (b) Six chords from trailing edge.

Hovering Flight of Caradonna-Tung Helicopter Rotor

Next, the Caradonna-Tung rotor in hovering flight, which was experimentally tested (Caradonna and Tung, 1981), was simulated. The rotor has two blades, and the blades are made of NACA0012 airfoil sections with an untwisted and non-tapered planform of an aspect ratio of six. The flow simulation is conducted at a tip Mach number of 0.877, a Reynolds number of 3.93 million, and a collective pitch angle of eight degrees. To improve the tip vortex resolution, the adaptive mesh refinement was utilized by using the non-dimensional Q-criterion. Mesh adaptation was conducted up to the second refinement level after the flow solution is fully converged.

Figure 5 shows comparison of the wake structures represented by the iso- λ_2 surface for the initial and adaptive meshes with the seventh-order WENO scheme in the off-body Cartesian mesh region. The far boundary size is five times of the rotor radius, and the typical minimum cell size at the initial off-body Cartesian mesh is $\Delta x = 0.05c$. In the case of the initial mesh solution, the wake vortices are emanated from the rotor blade tips, but are quickly diffused, even at seventh-order accuracy. After applying the adaptive mesh refinement scheme, it is observed the wake structures are much better resolved further downstream in the far wake by maintaining the shape and the strength along the adaptively refine cells.

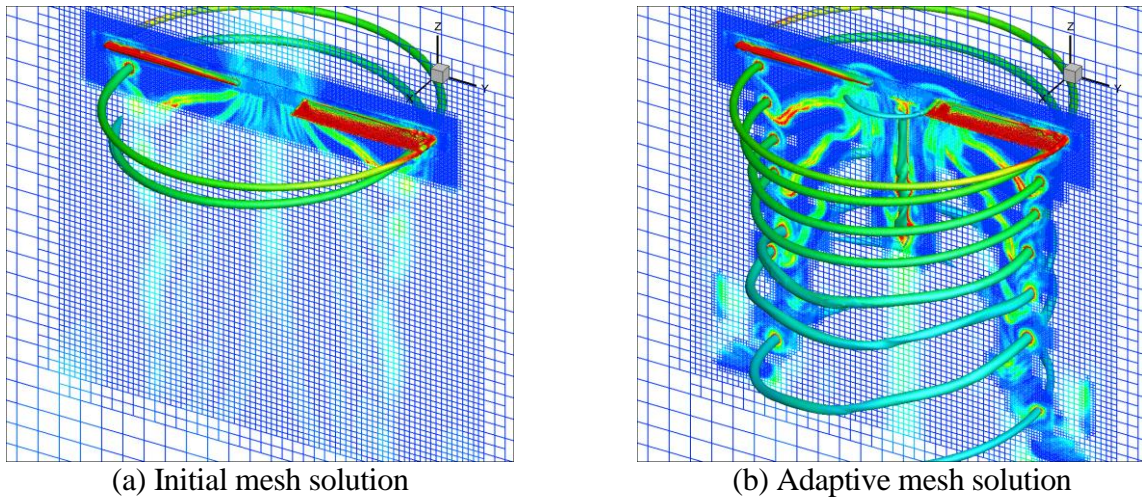


Figure 5. Predicted wake structures for Caradonna-Tung rotor with 7th-order accurate method. (a) Initial mesh solution; (b) Adaptive mesh solution.

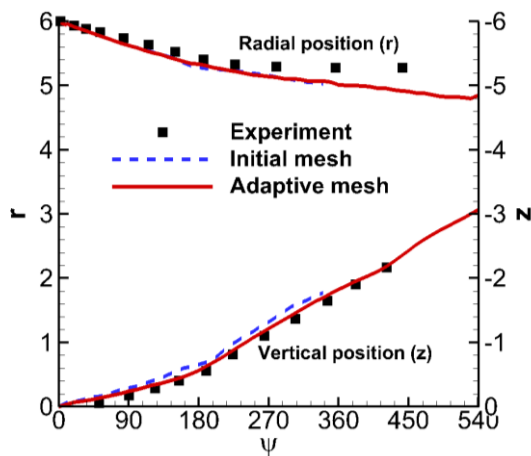


Figure 6. Predicted and experimental vortex trajectories of Caradonna-Tung rotor.

In Fig. 6, the predicted and experimental vortex trajectories of the Caradonna-Tung rotor in the hovering flight condition are compared between with and without the mesh adaptation. The trajectories are presented for both the radial and vertical positions for the rotor azimuthal angle from 0 to 540 degrees. In the initial mesh solution, the vortex trajectory was obtained only up to 350 degrees due to the numerical dissipation caused by the lack of fine cells. However, for the adaptive mesh solution, the vortex trajectory was well captured over 540 degrees, and are overall in good agreements with the experimental data for both the radial and vertical positions.

Conclusions

In the present study, a new mixed-type unstructured mesh flow solver is developed to obtain high-resolution for vortex-driven flows. For this purpose, prismatic/tetrahedral unstructured meshes are used in the near-body region, and adaptive Cartesian-based unstructured meshes are adopted in the off-body region. Unstructured prismatic/tetrahedral meshes enable to resolve the viscous shear flows near the body surface and easily handle complex geometric configurations. On the other hand in the off-body region, coupled high-order numerical scheme and solution-adaptive mesh refinement method were adopted to enhance the flow resolution by utilizing the nature of Cartesian meshes.

To assess the solution ability of the developed flow solver, an NACA0015 wing in steady flow and the Caradonna-Tung helicopter rotor in hovering flight were calculated. It was found that the present methodology is well capable of capturing and preserving the wake vortices. It was concluded that high-order scheme coupled with a proper adaptive mesh refinement method is indispensable elements for improving the off-body solution resolution containing highly vertical flow features.

Acknowledgments

This work was supported by the National Research Foundation of Korea (NRF) of grant funded by the Korean government (MSIP) (No. 2009-0083510). The authors also would like to acknowledge the support from National Research Foundation of Korea (NRF) Grant by the Korean government (No. 2011-0029094)

References

- Datta, A. and Johnson, W., (2008), An Assessment of the State-of-the-art in Multidisciplinary Aeromechanical Analysis. American Helicopter Society Technical Specialist's Meeting.
- Caradonna, F. X., Strawn, R. C., and Kholodar, D., (1988), An Experimental and Computational Study of Rotor-Vortex Interaction, *Vertica*, 12, pp. 315-327.
- Hariharan, N., Potsdam, M., and Wissink, A., (2012), Helicopter Rotor Aerodynamic Modeling in Hover Based on First-Principles: State-of-the-Art and Remaining Challenges. AIAA paper 2012-1066.
- Pulliam, T. H., and Jaspersen, D. C., (2009) Large Scale Aerodynamic Calculation on Pleiades. 21st International Conference on Parallel CFD.
- De Zeeuw, D. A., (1993), A Quadtree-Based Adaptively-Refined Cartesian-Grid Algorithm for Solution of the Euler Equations. PhD Thesis, University of Michigan.
- Kamkar, S., Wissink, A., Sankaran, V., and Jameson, A., (2011), Feature-driven Cartesian Adaptive Mesh Refinement for Vortex-dominated Flows, *J. of Computational Physics*, 230, pp. 6271-6298.
- Buning, P. G., et al, (2003), OVERFLOW User's Manual. NASA Langley Research Center.
- Wissink, A. M., Sitaraman, J., Sankaran, V., Mavriplis, D. J., and Pulliam, T. H., (2008), A Multi-Code Python-Based Infrastructure for Overset CFD with Adaptive Cartesian Grids. AIAA paper 2008-927.
- Mavriplis, D. J., and Venkatakrishnan, V., (1997), A Unified Multigrid Solver for the Navier-Stokes Equations on Mixed Element Meshes. *International Journal for Computational Fluid Dynamics*, 8, pp. 247-263.
- Hornung, R. D., Wissink, A. M., and Kohn, S. R., (2006), Managing Complex Data and Geometry in Parallel Structured AMR Applications. *Engineering with Computers*, 22, pp. 181-195.
- Pulliam, T. H., (1984), Euler and Thin-Layer Navier-Stokes Codes: ARC2D and ARC3D. Computational Fluid Dynamics User Workshop.

- Schluter, J. U., Wu, X., Weide, E., Hahn, S., Alonso, J. J., and Pitsch, H., (2005), Multi-Code Simulations: A Generalized Coupling Approach. AIAA paper 2005-4997.
- Aftosmis, M., J., (1997), Solution Adaptive Cartesian Grid Methods for Aerodynamic Flows with Complex Geometries. Von Karman Institute for Fluid Dynamics, Lecture Series 1997-02.
- McAllister, K., and Takahashi, R., (1991), NACA0015 Wing Pressure and Trailing Vortex Measurements. NASA Technical Paper 3151, AVSCOM Technical Report 91-A-003.
- Wissink, A. M, Kamkar, S., Pulliam, T. H., Sitaraman, J., and Sankaran, V., (2010), Cartesian Adaptive Mesh Refinement for Rotorcraft Wake Resolution. AIAA paper 2010-4554.
- Caradonna, F. X. and Tung, C., (1981), Experimental and Analytical Studies of a Model Helicopter Rotor in Hover. NASA TM 81232.